# Rainbow trapping of guided waves

Javier Polanco and Rosa M. Fitzgerald

*Department of Physics, University of Texas, El Paso, Texas 79968, USA*

Tamara A. Leskova and Alexei A. Maradudin[a)]

*Department of Physics and Astronomy, University of California, Irvine, California 92697, USA*

(Submitted April 8, 2011)
Fiz. Nizk. Temp. **37**, 1173–1180 (November 2011)

We study theoretically the propagation of a wave packet that is a superposition of three *s*-polarized guided waves with different frequencies in a planar waveguide consisting of a dielectric medium with a graded index of refraction, sandwiched between perfectly conducting walls. The electric field at each point within the waveguide is calculated, and it is shown that each of the constituent modes ceases to propagate at a specific distance along the waveguide that depends on its frequency and on the geometrical and material parameters defining the waveguide. This simple model displays the phenomenon of rainbow trapping of guided waves in an explicit fashion, without the use of a negative index metamaterial. © *2012 American Institute of Physics*. [doi: 10.1063/1.3672159]

There is currently a great deal of interest in slow light.[1] Experiments carried out involving ultracold atomic gases showed that light could be slowed down in traversing them[2] and even stopped.[3] The ability to slow light is of fundamental interest, but it also has practical uses in classical and quantum optical communication.[4]

It is therefore perhaps not surprising that with an increase in the use of surface plasmon polaritons in nanoscale devices attention has also begun to be directed at the possibility of slowing down these surface electromagnetic waves with the expectation that this will increase the scope of photonic devices based on them.

It has been known for some time[5] that the dispersion curve of a surface plasmon polariton propagating normal to the grooves and ridges of a classical metallic grating approaches the boundary of the one-dimensional first Brillouin zone defined by the period of the grating with zero slope, due to periodicity and time reversal symmetry. Thus the group velocity of the surface plasmon polariton slows down as the zone boundary is approached, and vanishes at the boundary itself. The slowing down of a surface Plasmon polariton wave packet by this mechanism was recently observed experimentally.[6]

This work was followed by several papers in which the slowing down of surface plasmon polaritons and guided waves was studied on the basis of a different approach. In a planar waveguide consisting of a dielectric layer sandwiched between two metals the number of modes than can be supported by this structure depends on the dielectric constant of the layer and its thickness. As the thickness of the dielectric layer decreases the number of modes supported by the waveguide decreases. Thus, if the waveguide does not have parallel walls, but instead has a thickness that decreases with increasing distance along it, at critical distances along the waveguide the number of modes decreases successively by one. These critical distances depend on the wavelengths of the modes. The group velocity of the mode that stops propagating at each of these distances is zero. When the thickness of the dielectric layer reaches the value where the waveguide no longer supports a mode, the group velocity of the only remaining waveguide mode at the corresponding distance along the waveguide is zero. If the waveguide is illuminated by polychromatic light consisting of several discrete wavelengths (a light rainbow), different light colors stop propagating at different positions along the waveguide. Thus, the light rainbow has been stopped and trapped.

This concept was used as the basis of an investigation by Tsakmakidis *et al*.[7] of the trapping of a guided wave packet in which a semi-infinite portion of the dielectric layer had a positive refractive index and parallel walls, while the remaining semi-infinite portion of the layer had a negative refractive index and a slowly decreasing thickness. The substrate and superstrate consisted of positive index dielectric materials. Trapping of the different frequency components of the guided wave packet at different points of the waveguide was predicted by these authors. This effect was observed experimentally by Zhao *et al*.[8]

A trapped rainbow was predicted and observed experimentally by Smolyaninova *et al*.[9] in a system of which a spherical metal structure was placed on a metal substrate. The air between the two metallic surfaces had a circularly symmetric structure whose thickness increased with increasing distance along the substrate from the point of its contact with the sphere. When illuminated from the side by polychromatic light, this structure displayed the trapping of its different wavelength components at specified distances along the substrate from the point of contact.

A variant of the tapered waveguide approach was used by Gan *et al*.[10] in a theoretical study of the trapping of surface plasmon polaritons. We have noted above that the dispersion curve of the lowest frequency branch of the dispersion relation for surface plasmon polaritons propagating normally to the grooves and ridges of a classical grating approaches the boundary of the first Brillouin zone defined by the period of the grating with a zero slope and a value (the cutoff frequency) that depends on the depth of the grooves. The deeper the grooves, the lower the cutoff frequency. Gan *et al*. considered a metallic lamellar grating the

 

depth of whose grooves increased linearly and slowly along the grating. When a surface plasmon polariton of a given frequency propagates along such a grating, it can reach a point along it at which the groove depth has a value such that an infinite grating with that groove depth would have a cut off frequency below that of the surface Plasmon polariton. At that point the surface wave ceases to propagate: its frequency falls in the region of the gap in the dispersion relation of an infinite grating with that groove depth. The surface plasmon is trapped at this point. If the incident surface plasmon polariton is a superposition of surface waves with different wavelengths, the different wavelength components will be trapped at different points along the grating.

What characterizes these studies of rainbow trapping is the absence of a quantitative theory underlying them. They are all based on the result that the narrower the thickness of a waveguide the fewer propagating modes it can support. While this result may be sufficient to estimate the points along the waveguide where these modes disappear one by one, it tells us nothing about the amplitudes of the propagating modes, it neglects the backscattering of the waves at the points where the group velocity vanishes, and it does not show how sharp the trapping phenomenon is, in view of the finite lengths of the structures studied.

In this paper we study the propagation of electromagnetic waves through a waveguide with a linearly graded dielectric constant, with a view to addressing the points raised in the preceding paragraph.

Taking the point of view that the use of a structure incorporating a negative index metamaterial is an unnecessary complication, the structure we study consists of a dielectric medium that occupies the region $-d<x_3<d$, and has a graded dielectric constant given by

$$\varepsilon(x_1)=\begin{cases}\varepsilon_\infty & x_1<-L\\ \dfrac{1}{2}(\varepsilon_\infty+1)-\dfrac{1}{2L}(\varepsilon_\infty-1)x_1 & -L<x_1<L\\ 1 & x_1>L\end{cases}. \quad (1)$$

For simplicity we assume that the region $x_3>d$ and $x_3<-d$ are filled with a perfect conductor. The electromagnetic field incident in this graded index waveguide from the region $x_1=-\infty$ is a superposition of $N$ $s$-polarized modes, each with a different frequency, supported by an infinitely long waveguide of constant thickness $2d$ and filled with a uniform dielectric medium whose dielectric constant is $\varepsilon_\infty$. The intensity of the electric field in this graded index waveguide will be calculated as a function of $x_1$ and $x_3$, from which the trapping of the incident rainbow can be observed.

The single nonzero component of the electric field in the waveguide, $E_2(x_1,x_3|\omega)$, satisfies the Helmholtz equation

$$\left(\frac{\partial^2}{\partial x_1^2}+\frac{\partial^2}{\partial x_3^2}+\varepsilon(x_1)\frac{\omega^2}{c^2}\right)E_2(x_1,x_3|\,\omega)=0 \quad (2)$$

in the domain $-\infty<x_1<\infty$, $-d<x_3<d$, subject to vanishing boundary conditions on the planes $x_3=\pm d$, and the continuity of $E_2(x_1,x_3|\,\omega)$ and $\partial E_2(x_1,x_3|\,\omega)/\partial x_1$ at $x_1=\pm L$.

We solve Eq. (2) by the method of the separation of variables. If we express $E_2(x_1,x_3|\,\omega)$ in the form

$$E_2(x_1,x_3|\,\omega)=f(x_1)g(x_3), \quad (3)$$

we find that $f(x_1)$ and $g(x_3)$ satisfy the equations

$$\frac{d^2}{dx_1^2}f(x_1)+\left[\varepsilon(x_1)\frac{\omega^2}{c^2}-\alpha^2\right]f(x_1)=0, \quad (4a)$$

$$\frac{d^2}{dx_3^2}g(x_3)+\alpha^2 g(x_3)=0, \quad (4b)$$

where $\alpha^2$ is the separation constant.

The solution of Eq. (4b) that vanishes at $x_3=-d$ is

$$g(x_3)=A\sin\alpha(x_3+d). \quad (5)$$

The requirement that $g(d)=0$ yields the result that

$$\alpha=\frac{n\pi}{2d},\quad n=1,2,3,\ldots. \quad (6)$$

Consequently we can write the solution of Eq. (4b) in

$$g_n(x_3)=A_n\sin\frac{n\pi}{2d}(x_3+d),\quad n=1,2,3,\ldots. \quad (7)$$

When Eq. (6) is substituted into Eq. (4a), we can write the resulting equation as

$$\frac{d^2}{dx_1^2}f_n(x_1)+\left[\varepsilon(x_1)\frac{\omega^2}{c^2}-\left(\frac{n\pi}{2d}\right)^2\right]f_n(x_1)=0. \quad (8)$$

We seek the solution of this equation in each of the three regions $(-\infty,-L)$, $(-L,L)$, and $(L,\infty)$.

$x_1<-L$: In this region Eq. (8) becomes

$$\frac{d^2}{dx_1^2}f_n(x_1)+\left[\varepsilon_\infty\frac{\omega^2}{c^2}-\left(\frac{n\pi}{2d}\right)^2\right]f_n(x_1)=0. \quad (9)$$

The solution of this equation is

$$f_n(x_1)=a_n^{(1)}\exp\left\{i\left[\varepsilon_\infty\frac{\omega^2}{c^2}-\left(\frac{n\pi}{2d}\right)^2\right]^{1/2}x_1\right\}+a_n^{(2)}\exp\left\{-i\left[\varepsilon_\infty\frac{\omega^2}{c^2}-\left(\frac{n\pi}{2d}\right)^2\right]^{1/2}x_1\right\}. \quad (10)$$

The first term can be regarded as an incident field, while the second term can be regarded as a reflected wave.

$-L<x_1<L$: In this region $f_n(x_1)$ satisfies the equation

$$\frac{d^2}{dx_3^2}f_n(x_1)+\left\{\frac{\omega^2}{c^2}\left[\frac{1}{2}(\varepsilon_\infty+1)-\frac{1}{2L}(\varepsilon_\infty-1)x_1\right]-\left(\frac{n\pi}{2d}\right)^2\right\}f_n(x_3)=0. \quad (11)$$

The solution of this equation is

$$f_n(x_1)=b_n^{(1)}Ai\left(\left(\frac{a\omega^2}{c^2}\right)^{1/3}(x_1-\beta_n)\right)+b_n^{(2)}Bi\left(\left(\frac{a\omega^2}{c^2}\right)^{1/3}(x_1-\beta_n)\right), \quad (12)$$

where

$$\beta_n = \frac{b}{a} - \frac{1}{a}\left(\frac{n\pi c}{2d\omega}\right)^2, \tag{13}$$

with

$$a = \frac{1}{2L}(\varepsilon_\infty - 1), \quad b = \frac{1}{2}(\varepsilon_\infty + 1). \tag{14}$$

In Eq. (12) $Ai(z)$ and $Bi(z)$ are two linearly independent Airy functions.[11]

$x_1 > L$: In this region the equation satisfied by $f_n(x_1)$ is

$$\frac{d^2}{dx_1^2} f_n(x_1) + \left[\frac{\omega^2}{c^2} - \left(\frac{n\pi}{2d}\right)^2\right] f_n(x_1) = 0. \tag{15}$$

The solution of this equation

$$f_n(x_1) = c_n \exp\left\{ i\left[\frac{\omega^2}{c^2} - \left(\frac{n\pi}{2d}\right)^2\right]^{1/2} x_1 \right\}, \tag{16}$$

which corresponds to a transmitted wave in this region. There is no wave incident from $x_1 = \infty$.

The boundary conditions satisfied by $f_n(x_1)$ are the continuity of $f_n(x_1)$ and of $df_n(x_1))/dx_1$ at $x_1 = -L$ and at $x_1 = L$. At $x_1 = -L$ we obtain the pair of equations

$$\begin{aligned} & a_n^{(1)} \exp\left\{ -i\left[\varepsilon_\infty \frac{\omega^2}{c^2} - \left(\frac{n\pi}{2d}\right)^2\right]^{1/2} L \right\} \\ & \quad + a_n^{(2)} \exp\left\{ i\left[\varepsilon_\infty \frac{\omega^2}{c^2} - \left(\frac{n\pi}{2d}\right)^2\right]^{1/2} L \right\} \\ & \quad = b_n^{(1)} Ai\left[\left(\frac{a\omega^2}{c^2}\right)^{1/3} (-L - \beta_n)\right] \\ & \quad + b_n^{(2)} Bi\left[\left(\frac{a\omega^2}{c^2}\right)(-L - \beta_n)\right]; \end{aligned} \tag{17a}$$

$$\begin{aligned} & i\left[\varepsilon_\infty \frac{\omega^2}{c^2} - \left(\frac{n\pi}{2d}\right)^2\right]^{1/2} \left\{ a_n^{(1)} \exp\left[ -i\left(\varepsilon_\infty \frac{\omega^2}{c^2} - \left(\frac{n\pi}{2d}\right)^2\right)^{1/2} L \right] \right. \\ & \quad \left. - a_n^{(2)} \exp\left[ i\left(\varepsilon_\infty \frac{\omega^2}{c^2} - \left(\frac{n\pi}{2d}\right)^2\right)^{1/2} L \right] \right\} \\ & \quad = \left(a\frac{\omega^2}{c^2}\right)^{1/3} \left\{ b_n^{(1)} Ai'\left[\left(\frac{a\omega^2}{c^2}\right)^{1/3} (-L - \beta_n)\right] \right. \\ & \quad \left. + b_n^{(2)} Bi'\left[\left(\frac{a\omega^2}{c^2}\right)^{1/3} (-L - \beta_n)\right] \right\}, \end{aligned} \tag{17b}$$

where the prime denotes differentiation with respect to argument. At $x_1 = L$ we obtain a second pair of equations

$$\begin{aligned} & b_n^{(1)} Ai\left[\left(a\frac{\omega^2}{c^2}\right)^{1/3} (L - \beta_n)\right] + b_n^{(2)} Bi\left[\left(a\frac{\omega^2}{c^2}\right)^{1/3} (L - \beta_n)\right] \\ & \quad = c_n \exp\left\{ i\left[\frac{\omega^2}{c^2} - \left(\frac{n\pi}{2d}\right)^2\right]^{1/2} L \right\}; \end{aligned} \tag{18a}$$

$$\begin{aligned} & \left(a\frac{\omega^2}{c^2}\right)^{1/3} \left[ b_n^{(1)} Ai'\left(\left(a\frac{\omega^2}{c^2}\right)^{1/3} (L - \beta_n)\right) \right. \\ & \quad \left. + b_n^{(2)} Bi'\left(\left(a\frac{\omega^2}{c^2}\right)^{1/3} (L - \beta_n)\right) \right] \\ & \quad = i\left[\frac{\omega^2}{c^2} - \left(\frac{n\pi}{2d}\right)^2\right]^{1/2} c_n \exp\left\{ i\left[\frac{\omega^2}{c^2} - \left(\frac{n\pi}{2d}\right)^2\right]^{1/2} L \right\}. \end{aligned} \tag{18b}$$

Equations (17) and (18) allow us to obtain the coefficients $a_n^{(2)}, b_n^{(1)}, b_n^{(2)}$, and $c_n$ in terms of $a_n^{(1)}$. Thus, we rewrite Eqs. (17) and (18) in the matrix form

$$\mathbf{M}^{(n)} \begin{pmatrix} a_n^{(2)} \\ b_n^{(1)} \\ b_n^{(2)} \\ c_n \end{pmatrix} = \begin{pmatrix} a_n^{(1)} \\ a_n^{(1)} \\ 0 \\ 0 \end{pmatrix} \tag{19}$$

where the nonzero elements of the matrix $\mathbf{M}^{(n)}$ are presented in the Appendix. We can then write

$$\begin{pmatrix} a_n^{(2)} \\ b_n^{(1)} \\ b_n^{(2)} \\ c_n \end{pmatrix} = \mathbf{N}^{(n)} \begin{pmatrix} a_n^{(1)} \\ a_n^{(1)} \\ 0 \\ 0 \end{pmatrix} \tag{20}$$

where $\mathbf{N}^{(n)}$ is the matrix inverse to $\mathbf{M}^{(n)}$. Therefore we have the results

$$a_n^{(2)} = \left(N_{11}^{(n)} + N_{12}^{(n)}\right) a_n^{(1)}; \tag{21a}$$

$$b_n^{(1)} = \left(N_{21}^{(n)} + N_{22}^{(n)}\right) a_n^{(1)}; \tag{21b}$$

$$b_n^{(2)} = \left(N_{31}^{(n)} + N_{32}^{(n)}\right) a_n^{(1)}; \tag{21c}$$

$$c_n = \left(N_{41}^{(n)} + N_{42}^{(n)}\right) a_n^{(1)}. \tag{21d}$$

We now assume that the portion of the waveguide in the region $x_1 < L$ is a single mode waveguide, i.e., we assume that $n = 1$. From Eq. (10) we see that we must have

$$\sqrt{\varepsilon_\infty}\frac{\omega}{c} > \frac{\pi}{2d} \tag{22}$$

and

$$\sqrt{\varepsilon_\infty}\frac{\omega}{c} < \frac{n\pi}{2d}, \quad n \geq 2. \tag{23}$$

These inequalities restrict $\omega/c$ to the interval

$$\frac{1}{\sqrt{\varepsilon_\infty}}\frac{\pi}{2d} < \frac{\omega}{c} < \frac{2}{\sqrt{\varepsilon_\infty}}\frac{\pi}{2d}. \tag{24}$$

At the same time we wish to have no propagating modes in the region $x_1 > L$. From Eq. (16) we see that for this to be the case we must satisfy the inequality

$$\frac{\omega}{c} < \frac{\pi}{2d}. \tag{25}$$

We will assume that $\varepsilon_\infty$ is sufficiently greater than unity that $2/\sqrt{\varepsilon_\infty}$ is smaller than unity. Therefore the right-hand inequality in Eq. (24) is more restrictive than the inequality (25). If we introduce the dimensionless frequency $\Omega$ by

$$\frac{\omega}{c} = \Omega \frac{\pi}{2d}, \tag{26}$$

the inequalities (24) become

$$\frac{1}{\sqrt{\varepsilon_\infty}} < \Omega < \frac{2}{\sqrt{\varepsilon_\infty}}. \tag{27}$$

We will choose for $\varepsilon_\infty$ the value that corresponds to silicon, namely $\varepsilon_\infty = 12$. With this value of $\varepsilon_\infty$, the inequalities (27) become

$$0.2887 < \Omega < 0.5774. \tag{28}$$

With these results in hand we will assume that the incident electric field is a wave packet formed by the superposition of $N=3$ modes whose frequencies $\Omega_j (j=1,2,3)$ satisfy the inequalities (28), namely

$$\Omega_1 = 0.35, \quad \Omega_2 = 0.45, \quad \Omega_3 = 0.55. \tag{29}$$

It now remains to determine the half-width $d$ of the waveguide and the length $2L$ of the portion filled with the graded index dielectric medium. We do this by first noting that the wavelength $\lambda$ of the mode of the frequency $\omega$ in the region $x_1 < -L$ is obtained from the relation

$$\sqrt{\varepsilon_\infty}\frac{\omega}{c} = \frac{2\pi}{\lambda}, \tag{30}$$

so that

$$\lambda = \frac{4d}{\sqrt{\varepsilon_\infty}\Omega}. \tag{31}$$

where we have used the relation (26). The wavelengths corresponding to the frequencies $\Omega_1$, $\Omega_2$, $\Omega_3$ are therefore given by

$$\lambda_1 = 3.2991d; \tag{32a}$$

$$\lambda_2 = 2.5660d; \tag{32b}$$

$$\lambda_3 = 2.0995d. \tag{32c}$$

We will choose for $\lambda_1$ the value $\lambda_1 = 0.6328\,\mu$m. It follows from Eqs. (32) that $\lambda_2 = 0.4922\,\mu$m, and $\lambda_3 = 0.4027\,\mu$m. From the same equations we find that $d = 0.1918\,\mu$m.

In choosing a value for $L$ we wish to make the ratio $d/L$ sufficiently small that the dielectric constant within the region $-L < x_1 < L$ of the waveguide is changing slowly with $x_1$. We have chosen the value $L = 6\,\mu$m, which yields the ratio $d/L = 0.032$.

The incident electric field in the region $x_1 < -L$ can be written in the form

$$E_2(x_1,x_3)_{\text{inc}} = \sum_{j=1}^{3} a_1^{(1j)} \sin\frac{\pi}{2d}(x_3+d) \times \exp\left\{ i\frac{\pi}{2d}\left[\varepsilon_\infty \Omega_j^2 - 1\right]^{1/2} x_1 \right\}, \tag{33}$$

where $\omega_j/c = \Omega_j(\pi/2d)$. Since the scattering problem is a linear one, the reflected field in the region $x_1 < -L$ is given by

$$E_2(x_1,x_3)_{\text{ref}} = \sum_{j=1}^{3} \left(N_{11}^{(1j)} + N_{12}^{(1j)}\right) a_1^{(1j)} \times \sin\frac{\pi}{2d}(x_3+d) \exp\left\{ -i\frac{\pi}{2d}\left[\varepsilon_\infty \Omega_j^2 - 1\right]^{1/2} x_1 \right\}. \tag{34}$$

Similarly, the transmitted field in the region $x_1 > L$ is

$$E_2(x_1,x_3)_{\text{tr}} = \sum_{j=1}^{3} \left(N_{41}^{(1j)} + N_{42}^{(1j)}\right) a_1^{(1j)} \times \sin\frac{\pi}{2d}(x_3+d) \exp\left\{ i\frac{\pi}{2d}\left[\Omega_j^2 - 1\right]^{1/2} x_1 \right\}. \tag{35}$$

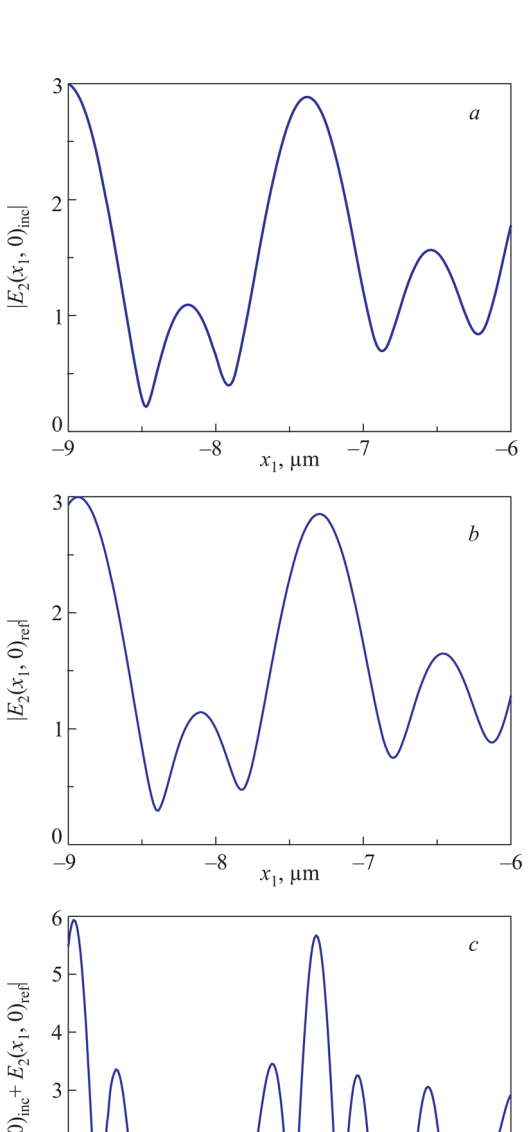


FIG. 1. Plots of $|E_2(x_1,0)_{\text{inc}}|$ (*a*), $|E_2(x_1,0)_{\text{ref}}|$ (*b*), and $|E_2(x_1,0)_{\text{inc}} + E_2(x_1,0)_{\text{ref}}|$ (*c*) in the region $x_1 < -L$ of the waveguide.

The field inside the region $-L<x_1<L$ containing the graded index material is

$$E_2(x_1,x_3)_{\rm gr}=\sum_{j=1}^{3}a_1^{(1j)}\sin\frac{\pi}{2d}(x_3+d)\times\left\{\left(N_{21}^{(1j)}+N_{22}^{(1j)}\right)Ai\left[\left(a\frac{\omega_j^2}{c^2}\right)^{1/3}(x_1-\beta_1^{(j)}\right]+\left(N_{31}^{(1j)}+N_{32}^{(1j)}\right)Bi\left[\left(a\frac{\omega_j^2}{c^2}\right)^{1/3}(x_1-\beta_1^{(j)}\right]\right\}. \tag{36}$$

The matrix elements $N_{mn}^{(1j)}$ are the elements of the matrix inverse to the matrix $\mathbf{M}^{(n)}$ whose elements are given in the Appendix, when $n=1$ and $\omega$ is replaced by $\omega_j=\Omega_j(\pi c/2d)$.

The Airy functions $Ai(z)$ and $Bi(z)$ are both oscillatory functions of $z$ for negative values of $z$, and have a descending or ascending exponential behavior, respectively, for positive values of $z$. Therefore, we can expect that the mode whose frequency is $\omega_j$ in the incident field will stop propagating at the position $x_1^{(j)}$ given by

$$x_1^{(j)}=\beta_1^{(j)}=\frac{1}{a}\left[b-\left(\frac{\pi c}{2d\omega_j}\right)^2\right]=\frac{1}{a}\left(b-\frac{1}{\Omega_j^2}\right). \tag{37}$$

With our assumption that $\varepsilon_\infty=12$, we find from Eqs. (14) that

$$a=\frac{5.5}{L},\quad b=6.5. \tag{38}$$

With these values of $a$ and $b$, and the values of $\Omega_j$ given by Eqs. (29), we find that the stopping points $x_1^{(j)}$ are

$$x_1^{(1)}=-0.3024L=-1.8144\mu\text{m}; \tag{39a}$$

$$x_1^{(2)}=0.2480L=-1.7037\mu\text{m}; \tag{39b}$$

$$x_1^{(3)}=0.5805L=-3.4845\mu\text{m}, \tag{39c}$$

where the second equality in each case follows from our assumption that $L=6\,\mu$m.

We illustrate the preceding results by numerical calculations of the electric field and its intensity in each of the regions $x_1<-L$, $-L<x_1<L$, and $x_1>L$. In these

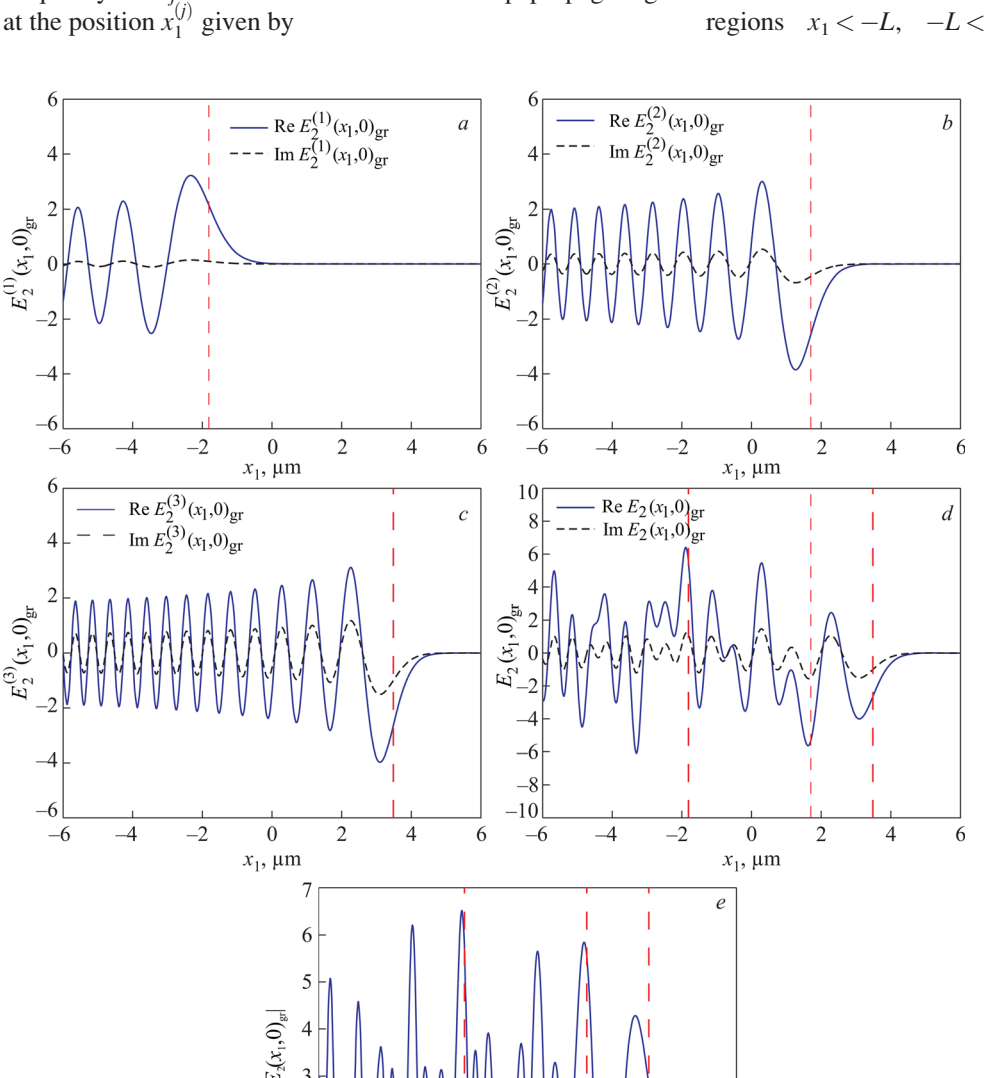


FIG. 2. (*a*)–(*c*) Plots of the real and imaginary parts of $E_2^{(1)}(x_1,0)_{\rm gr}$, $E_2^{(2)}(x_1,0)_{\rm gr}$, and $E_2^{(3)}(x_1,0)_{\rm gr}$, respectively. (*d*) Plots of the real and imaginary parts of $[E_2(x_1,0)_{\rm gr}]$. (*e*) A plot of $|E_2(x_1,0)_{\rm gr}|$. The dashed vertical lines indicate the values of $x_1^{(j)}(j=1,2,3)$.

calculations, to simplify the resulting figures, we have set $x_3 = 0$ and have assumed that each amplitude $a_1^{(1j)}(j = 1,2,3)$ is equal to unity.

In Fig. 1 we plot $|E_2(x_1,0)_{\text{inc}}|$ $(a)$, $|E_2(x_1,0)_{\text{ref}}|$ $(b)$, and the magnitude of the total field $|E_2(x_1,0)_{\text{inc}}+E_2(x,0)_{\text{ref}}|$ $(c)$ in the region $x_1<-L$. The shorter period oscillations observed in $(c)$ compared with those in $(a)$ and $(b)$ arise from the interference of the incident and reflected waves in this region of the waveguide. It is seen from these results that the intensity of the reflected field is comparable to the intensity of the incident field.

More interesting is the behavior of the electric field in the region $-L<x_1<L$ of the waveguide occupied by the graded refractive index medium. In Figs. 2(*a*)–2(*c*) we plot the real and imaginary parts of $E_2^{(1)}(x_1,0)_{\text{gr}}$, $E_2^{(2)}(x_1,0)_{\text{gr}}$, and $E_2^{(3)}(x_1,0)_{\text{gr}}$, respectively, as functions of $x_1$. It is seen that each of these fields decreases rapidly to zero exponentially as $x_1$ increases past the distances $x_1^{(3)}$, respectively. This is the rainbow trapping effect. However, a stepwise decrease in the real and imaginary parts of the total electric field at each of these distances is less clearly present in Fig. 2(*d*), although a trend to smaller values of $\text{Re}E_2(x_1,0)_{\text{gr}}$ as $x_1$ crosses $x_1^{(j)}$ $(j = 1,2,3)$ is seen. The same can be said of the plot of $|E_2(x_1,0)_{\text{gr}}|$ presented in Fig. 2(*e*).

Propagation of the electric field stops at $x_1 \approx x_1^{(3)}$, and the magnitude of the field decreases exponentially for $x_1$ greater than $x_1^{(3)}$.

The magnitude of the electric field in the region $x_1 > L$, $|E_2(x_1,0)_{\text{tr}}|$, also decreases exponentially with increasing $x_1$, as can be seen from the result plotted in Fig. 3.

We have studied the propagation of a wave packet consisting of a superposition of three *s*-polarized guided waves with different frequencies in a planar waveguide consisting of a dielectric medium with a graded index of refraction sandwiched between perfectly conducting walls. This simple model system displays features observed in earlier studies of the rainbow trapping of guided waves, in particular that each frequency component of the incident wave packet stops propagating at a specific distance along the waveguide that depends on its frequency (its color) and on the material and geometrical parameters defining the waveguide. It also shows some features not discussed in these earlier studies. These include the strong reflection of the incident field from the waveguide, which appears to be due to the cessation of transmission of the waves comprising that field at specific distances along the waveguide, and the fact that the trapping phenomenon is not sharp but displays an exponential decay of the electric field strength on the transmission side at each of these distances. An attractive feature of the model system studied is that its properties can be studied analytically rather than purely studied numerically.

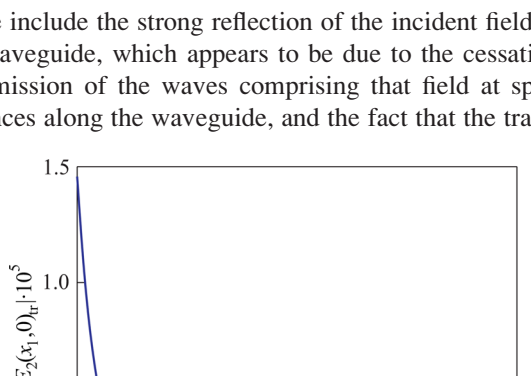


FIG. 3. A plot of $|E_2(x_1,0)_{tr}|$ in the region $x_1 > L$ of the waveguide.

## APPENDIX

The nonzero elements of the matrix $\mathbf{M}^{(n)}$ entering Eq. (19) are:

$$M_{11}^{(n)} = -\exp\left\{i2\left[\varepsilon_\infty \frac{\omega^2}{c^2} - \left(\frac{n\pi}{2d}\right)^2\right]^{1/2} L\right\}; \tag{A1}$$

$$M_{12}^{(n)} = \exp\left\{i\left[\varepsilon_\infty \frac{\omega^2}{c^2} - \left(\frac{n\pi}{2d}\right)^2\right]^{1/2} L\right\} \times Ai\left[\left(a\frac{\omega^2}{c^2}\right)^{1/3}(-L-\beta_n)\right]; \tag{A2}$$

$$M_{13}^{(n)} = \exp\left\{i\left[\varepsilon_\infty \frac{\omega^2}{c^2} - \left(\frac{n\pi}{2d}\right)^2\right]^{1/2} L\right\} \times Bi\left[\left(a\frac{\omega^2}{c^2}\right)^{1/3}(-L-\beta_n)\right]; \tag{A3}$$

$$M_{21}^{(n)} = \exp\left\{i2\left[\varepsilon_\infty \frac{\omega^2}{c^2} - \left(\frac{n\pi}{2d}\right)^2\right]^{1/2} L\right\}. \tag{A4}$$

$$M_{22}^{(n)} = \exp\left\{i\left[\varepsilon_\infty \frac{\omega^2}{c^2} - \left(\frac{n\pi}{2d}\right)^2\right]^{1/2} L\right\} \times \frac{\left(a\frac{\omega^2}{c^2}\right)^{1/3}}{i\left[\varepsilon_\infty \frac{\omega^2}{c^2} - \left(\frac{n\pi}{2d}\right)^2\right]^{1/2}} Ai'\left[\left(a\frac{\omega^2}{c^2}\right)^{1/3}(-L-\beta_n)\right]; \tag{A5}$$

$$M_{23}^{(n)} = \exp\left\{i\left[\varepsilon_\infty \frac{\omega^2}{c^2} - \left(\frac{n\pi}{2d}\right)^2\right]^{1/2} L\right\} \times \frac{\left(a\frac{\omega^2}{c^2}\right)^{1/3}}{i\left[\varepsilon_\infty \frac{\omega^2}{c^2} - \left(\frac{n\pi}{2d}\right)^2\right]^{1/2}} Bi'\left[\left(a\frac{\omega^2}{c^2}\right)^{1/3}(-L-\beta_n)\right]; \tag{A6}$$

$$M_{32}^{(n)} = Ai\left[\left(a\frac{\omega^2}{c^2}\right)^{1/2}(L-\beta_n)\right]; \tag{A7}$$

$$M_{33}^{(n)} = Bi\left[\left(a\frac{\omega^2}{c^2}\right)^{1/3}(L-\beta_n)\right]; \tag{A8}$$

$$M_{34}^{(n)} = -\exp\left\{i\left[\frac{\omega^2}{c^2} - \left(\frac{n\pi}{2d}\right)^2\right]^{1/2} L\right\}; \tag{A9}$$

$$M_{42}^{(n)} = \frac{\left(a\frac{\omega^2}{c^2}\right)^{1/3}}{i\left[\frac{\omega^2}{c^2} - \left(\frac{n\pi}{2d}\right)^2\right]^{1/2}} Ai'\left[\left(a\frac{\omega^2}{c^2}\right)^{1/3}(L-\beta_n)\right]; \quad \text{(A10)}$$

$$M_{43}^{(n)} = \frac{\left(a\frac{\omega^2}{c^2}\right)^{1/3}}{i\left[\frac{\omega^2}{c^2} - \left(\frac{n\pi}{2d}\right)^2\right]^{1/2}} Bi'\left[\left(a\frac{\omega^2}{c^2}\right)^{1/3}(L-\beta_n)\right]; \quad \text{(A11)}$$

$$M_{44}^{(n)} = -\exp\left\{i\left[\frac{\omega^2}{c^2} - \left(\frac{n\pi}{2d}\right)^2\right]^{1/2} L\right\}. \quad \text{(A12)}$$

We dedicate this paper to the memory of E. A. Kaner on the occasion of his 80th birthday. Gone, but not forgotten.

The research of J.P. and R.M.F. was supported in part by NOAA Educational Partnership Program for Minority Serving Institutions (EPP/MSI) Cooperative Agreement NAITAE1623. The research of T.A.L. and A.A.M. was supported in part by AFRL contract FA9453-08-C-0230.

[a]Email: aamaradu@uci.edu

[1]R. W. Boyd and D. J. Gauthier, Science **326**, 1074 (2009).
[2]L. V. Hau, S. F. Harris, Z. Dutton, and C. H. Behroozi, Nature **397**, 594 (1999).
[3]C. Liu, Z. Dutton, C. H. Behroozi, and L. V. Hau, Nature **409**, 490 (2001).
[4]M. L. Povinelli, Nat. Phys. **2**, 735 (2006).
[5]B. Laks, D. L. Mills, and A. A. Maradudin, Phys. Rev. B **23**, 4965 (1981).
[6]M. Sandtke and L. Kuipers, Nature Photon. **1**, 573 (2007).
[7]K. L. Tsakmakidis, A. D. Boardman, and O. Hess, Nature **450**, 397 (2007).
[8]X. P. Zhao, W. Luo, J. X. Huang, Q. H. Fu, K. Song, X. C. Cheng, and C. R. Luo, Appl. Phys. Lett. **95**, 071111 (2009).
[9]V. N. Smolyannova, I. I. Smolyaninov, A. V. Kildshev, and V. M. Shalaev, Appl. Phys. Lett. **96**, 211121 (2010).
[10]Q. Gan, Y. J. Ding, and F. J. Bartoli, Phys. Rev. Lett. **102**, 056801 (2009).
[11]*Handbook of Mathematical Functions*, edited by M. Abramowitz and I. A. Stegun (Dover, New York, 1972), p. 446.

This article was published in English in the original Russian journal. Reproduced here with stylistic changes by AIP.